

PROCEEDINGS OF SPIE

[SPIDigitalLibrary.org/conference-proceedings-of-spie](https://spiedigitallibrary.org/conference-proceedings-of-spie)

ULTIMATE-Subaru: GLAO preliminary design overview

Yosuke Minowa, Yoshito Ono, Yoko Tanaka, Hiroshige
Yoshida, Koki Terao, et al.

Yosuke Minowa, Yoshito Ono, Yoko Tanaka, Hiroshige Yoshida, Koki Terao, Yusei Koyama, Sadman Ali, Ichi Tanaka, Takashi Hattori, Hirofumi Okita, Yutaka Hayano, Shin Oya, Kentaro Motohara, Kenshi Yanagisawa, Michitoshi Yoshida, Masayuki Akiyama, Tadayuki Kodama, Hajime Ogane, Masahiro Konishi, Noelia Martinez Rey, Nicholas Herral, Céline d'Orgeville, François Rigaut, Israel Vaughn, David Chandler, Dionne Haynes, Warrick Schofield, Shiang-Yu Wang, Chi-Yi Chou, Masahiko Kimura, "ULTIMATE-Subaru: GLAO preliminary design overview," Proc. SPIE 12185, Adaptive Optics Systems VIII, 1218521 (29 August 2022); doi: 10.1117/12.2629749

SPIE.

Event: SPIE Astronomical Telescopes + Instrumentation, 2022, Montréal, Québec, Canada

ULTIMATE-Subaru: GLAO preliminary design overview

Yosuke Minowa^a, Yoshito Ono^a, Yoko Tanaka^a, Hiroshige Yoshida^a, Koki Terao^a, Yusei Koyama^a, Sadman Ali^a, Ichi Tanaka^a, Takashi Hattori^a, Hirofumi Okita^a, Yutaka Hayano^a, Shin Oya^b, Kentaro Motohara^{b,d}, Kenshi Yanagisawa^b, Michitoshi Yoshida^b, Masayuki Akiyama^c, Tadayuki Kodama^c, Hajime Ogane^c, Masahiro Konishi^d, Noelia Martinez Rey^e, Nicholas Herrald^e, Céline d'Orgeville^e, François Rigaut^e, Israel Vaughn^e, David Chandler^e, Dionne Haynes^e, Warrick Schofield^e, Shiang-Yu Wang^f, Chi-Yi Chou^f, and Masahiko Kimura^f

^aSubaru Telescope, National Astronomical Observatory of Japan, 650 North A'ohoku Place, Hilo, HI, 96720

^bNational Astronomical Observatory of Japan, 2-21-1 Osawa, Mitaka, Tokyo, 181-8588, Japan

^cAstronomical Institute, Tohoku University, Aramaki, Aoba-ku, Sendai 980-8578, Japan

^dInstitute of Astronomy, Graduate School of Science, The University of Tokyo, 2-21-1 Osawa, Mitaka, Tokyo 181-0015, Japan

^eResearch School of Astronomy and Astrophysics, Australian National University, Canberra, ACT 2611, Australia

^fAcademia Sinica, Institute of Astronomy and Astrophysics, P. O. Box 23-141, Taipei, Taiwan

ABSTRACT

ULTIMATE-Subaru* is a next facility instrumentation program of the Subaru Telescope. The goal of this project is to extend the wide-field capability of the Subaru telescope to near-infrared (NIR) wavelength, by developing a wide-field ground-layer adaptive optics (GLAO) system and wide-field NIR instruments. The GLAO system will uniformly improve the image quality up to 20-arcmin field of view in diameter by correcting for the ground-layer turbulence. The expected image quality after the GLAO correction is FWHM $\sim 0''.2$ in K-band under moderate seeing conditions. In this presentation, we present preliminary design overview of the GLAO system at the Cassegrain focus, which consist of an adaptive secondary mirror, wavefront sensor unit, a laser guide star facility, and control system. We also present the prototyping activities to validate the selected design of the GLAO system.

Keywords: Adaptive Optics, GLAO, Wide field, Near-infrared

1. INTRODUCTION

The Subaru telescope has started a new operation concept called "Subaru 2" in 2022. In this concept, we put more weight on the wide-field survey observations. The Subaru telescope has been operating a wide-field survey instruments in optical wavelength at its prime focus (HSC¹ and PFS²). ULTIMATE-Subaru is a project to develop next facility instruments at the Subaru Telescope that expand the wide-field survey capability to near-infrared (NIR) wavelength. In this project, we will develop wide-field NIR instruments and a Ground-Layer Adaptive Optics (GLAO) that will enhance the sensitivity and spatial resolution of the NIR observations. The GLAO can uniformly improve the image quality over a wide field of view by correcting for the ground-layer turbulence. In 2018, we have successfully completed a conceptual design review of the GLAO system of ULTIMATE-Subaru. We demonstrated the feasibility of developing the GLAO system with the field of view (FoV) up to 20 arcmin at the Cassegrain focus. We also conducted comprehensive statistical simulation that predicts the GLAO performance using more than 1,000 Cn² profiles based on the actual measurements at Maunakea with varying the observing

Further author information: (Send correspondence to YM)

YM: E-mail: minoways@naoj.org, Telephone: +1 808 934 5905

*<https://ultimate.naoj.org/english/index.html>

conditions such as zenith distance, sodium return, and sky background.³ We confirmed that the GLAO can improve the image quality by a factor of two at the most of the seeing conditions and the median seeing after the GLAO correction is expected to be ~ 0.2 arcsec in *K* band. The main science instrument proposed to use with the GLAO is WFI,⁴ which is a NIR (0.9–2.5 μm) wide-field imager covering 14×14 arcmin² FoV at the Cassegrain focus. There is also a plan to feed the GLAO correction to the existing wide-field multi-object spectrograph, MOIRCS,⁵ at the Nasmyth IR focus. The conceptual design of the science instruments has been successfully completed in mid-2021.

The primary scientific goal of the ULTIMATE-Subaru project is to perform square-degree scale imaging and spectroscopic surveys in near-infrared wavelength by taking advantage of the enhanced sensitivity with the GLAO, aiming to reveal the birth, growth, and death of galaxies across cosmic time and environment. There are also plans to conduct high-cadence transient/astrometric survey observations especially at the region around the Galactic Center by utilizing the enhanced spatial resolution with the GLAO.

ULTIMATE-Subaru project is led by the Subaru telescope in collaboration with the Australian National University (ANU), Tohoku University, Academia Sinica Institute of Astronomy and Astrophysics (ASIAA), the University of Tokyo, and National Astronomical Observatory of Japan (NAOJ). The GLAO is currently in a preliminary design phase, which is expected to complete in late 2022. The Subaru telescope is responsible for the overall GLAO design, ANU is responsible for the designs of the Wavefront Sensor (Section 3.3) and the Laser Guide Star (Section 3.4) subsystems, and Tohoku University is responsible for the prototyping activities (Section 4). The conceptual design of the science instrument has been conducted by the collaboration among NAOJ, ASIAA, and the University of Tokyo.

In this paper, we briefly summarize the GLAO system requirements derived from the associated science cases (Section 2) and present an overview of the preliminary design of the GLAO system (Section 3). Finally, we introduce the prototyping activities that demonstrate the feasibility and performance of the selected GLAO design (Section 4).

2. GLAO SYSTEM REQUIREMENTS

Top-Level science requirements of ULTIMATE-Subaru have been derived from the science use cases considering a large survey program using 300-360 nights for 5 years based on the existing frame work of the Subaru Strategic Program (SSP). Table 1 shows a summary of the top-level science requirements for WFI+GLAO at the Cassegrain focus.

Table 1. Summary of the top-level science requirements for WFI+GLAO at the Cassegrain focus.

Science Wavelength Coverage	0.9 – 2.5 μm
Science FoV	$> 14 \times 14$ arcmin ²
Image Quality (FWHM)	$< 0''.25$ at J (20%-ile), $< 0''.25$ at K (50%-ile)
Image Quality (EE50 ^a)	$< 0''.50$ at J (20%-ile), $< 0''.50$ at K (50%-ile)
Image Uniformity	$\Delta\text{EE}50 < 10$ %
Sky Coverage	> 90 %
Overhead	Observing Efficiency > 80 %, Exposure Overhead < 20 %

^a Aperture diameter to contain 50 % energy.

Based on the GLAO end-to-end numerical simulation³ and optical system models of the telescope and WFI,⁶ we developed a system performance model of GLAO + WFI and derived the GLAO system specification that satisfies the top-level science requirements as well as the interface and operational requirements. Table 2 shows a summary of the derived specification of the GLAO system at the Cassegrain focus. The number of actuators, control modes, NGSs, LGSs were optimized by numerical simulations^{3,7} so as to uniformly provide the required image quality over the largest science FoV ($\sim 14' \times 14'$) at the Cassegrain focus.

Despite the large science FoV of WFI covering 14×14 arcmin², the GLAO system is designed to allow the LGSs to be located within the nominal science FoV so as to improve the GLAO corrected image quality for the

science cases that do not require the full field of view WFI. We expect that the GLAO corrected image quality can be ~ 1.5 times better by narrowing the size of the LGS asterism from 10 arcmin to 2 arcmin in radius.³

Table 2. Summary of the GLAO system specification at the Cassegrain focus.

Deformable Mirror		
Number of actuators	924	
Control modes	> 350 KL modes	
Guide Star		
Natural Guide Star (NGS)	Up to 4 ($r < 18$ mag)	
Laser Guide Star (LGS)	4 (~ 720 photons/sec/cm ² for each)	
Wavefront Sensor (WFS)		
	NGS	LGS
Number of WFS	3 (tip/tilt) + 1 (tip/tilt/focus)	4
Patrol FoV (Radius)	7-10 arcmin (outside of Science FoV)	2 – 10 arcmin (including Narrow-Field mode)
Sub-apertures	1 × 1 or 2 × 2	32 × 32
Frame rate	< 500 Hz	500 Hz

3. GLAO PRELIMINARY DESIGN OVERVIEW

In this section, we discuss the preliminary design of the GLAO system to feed the corrected light to the Cassegrain focus where the maximum FoV up to 20 arcmin in diameter is available.

3.1 System Architecture

The overall GLAO system architecture is shown in Figure 1. The GLAO system can be decomposed into four main subsystems: the Adaptive Secondary Mirror (ASM), the Wavefront sensor (WFS) unit, the Laser Guide Star Facility (LGSF), and the control system. The GLAO system will be highly integrated into the Subaru telescope. The ASM will be installed to the telescope main optical path instead of the existing infrared secondary mirror. The LGSF, which is further decomposed into the laser generation, beam diagnostics, beam transfer, and beam launching parts, will be integrated into the telescope structure to launch the laser beams from the side of the primary mirror toward the same pointing as the telescope. The WFS unit, which consists of the LGS and the NGS WFSs, is installed at the Cassegrain focus together with the science instrument WFI. The WFS acquires the light from the guide stars without blocking the NIR science path to maximize the throughput of WFI. The control system is composed by the instrument control (OBCP) and the real-time control (RTC) systems. The RTC is responsible for the GLAO main control loop in real-time manner, while the OBCP is responsible for the GLAO non real-time operation by interacting with the operators and the telescope control system (TSC) through the observation control system (OCS).

3.2 Adaptive Secondary Mirror

The Adaptive Secondary Mirror (ASM) is a large secondary mirror which is 1,265 mm in diameter and is equipped with 924 actuators for AO correction. The ASM utilizes the same technology as the previous generation deformable secondary mirrors developed by the AdOptica consortium in Italy,⁸ but with implementing the most recent improvements especially in the actuator control being adopted for the deformable secondary mirrors being designed for 30-m class telescopes.⁹ Figure 2 shows the adopted design for the Subaru ASM. The ASM unit will be installed in the existing infrared secondary mirror (IRM2) mount being used at the Subaru telescope for infrared observations. The mirror and mirror cell of the IRM2 will be replaced by the ASM to provide the AO corrected light to the Nasmyth and Cassegrain foci of the Subaru telescope. Since we regularly exchange the top unit of the Subaru telescope between the prime-focus instrument (HSC and PFS) and the secondary mirror, the ASM is designed to withstand the frequent exchange work, especially to keep the thin shell mirror protected

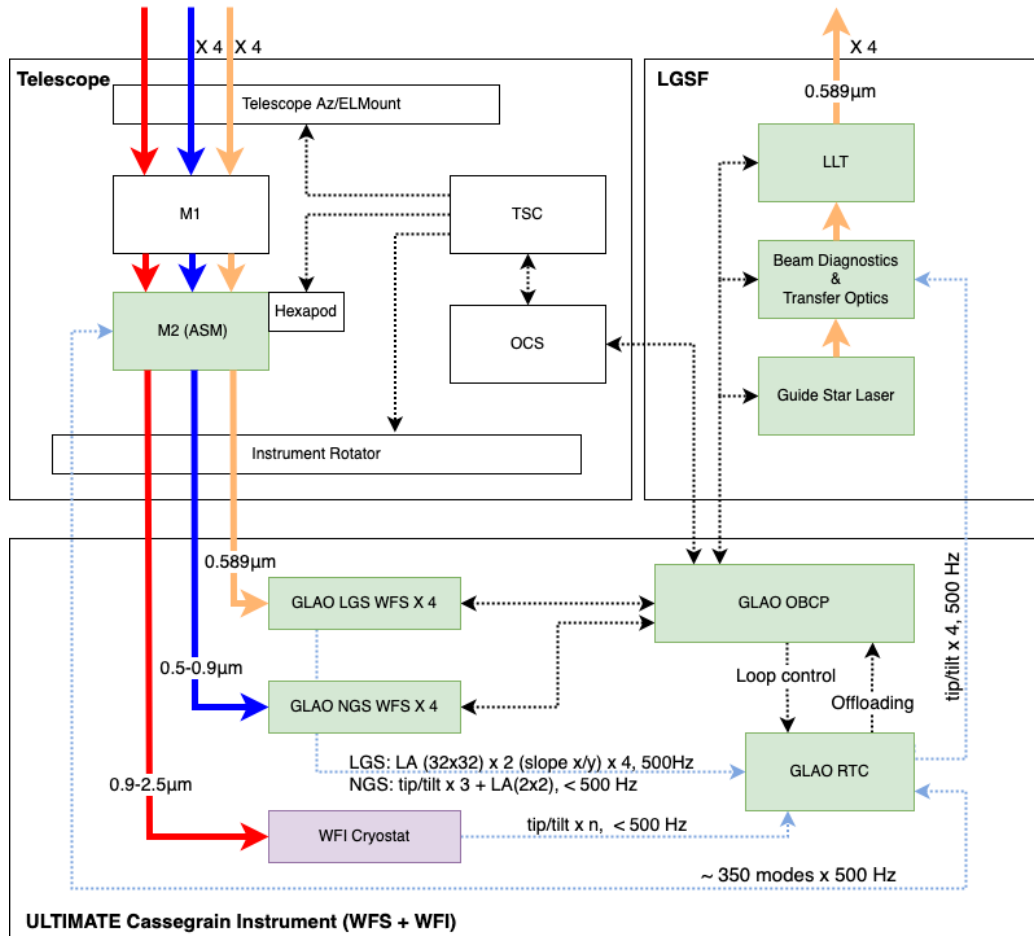


Figure 1. The GLAO system architecture along with the telescope sub-systems. The GLAO sub-systems are shown in green blocks. The diagram also shows how the GLAO sub-systems and the telescope sub-systems interact each other. Blue lines represent real-time signals. Black lines represent non real-time signals.

during the exchange. The ASM control electronics onboard the IRM2 is equipped with a battery to keep the ASM unit powered even when the main power cable is disconnected for the exchange work.

The ASM uses the large convex thin shell mirror with the thickness of 2 mm. Since the procurement of the thin shell mirror requires long lead time, the design of the ASM has been most advanced compared to the other GLAO sub-systems. We have completed the final design of the ASM and started a production process of the thin shell mirror. While we are starting the production phase of the ASM unit, we are finalizing the calibration plan for the ASM to evaluate the optical performance and to conduct functional test with the WFS unit. We are planning to develop a dedicated equipment to do the calibrations in the laboratory before installing the ASM to the telescope. The details of the adopted ASM design and its calibration strategies are reported by Oya, S. et al. in this conference.¹⁰

3.3 Wavefront Sensor Unit

The design of the GLAO WFS unit has been developed for the Cassegrain focus. The WFS unit consists of the LGS and the NGS WFS layers on top of the science instrument (WFI) at the Cassegrain focus. Figure 3 shows the configuration of the WFS layers located above the WFI cryostat. The WFS unit is attached to the telescope Cassegrain focus together with WFI, where the field rotations is compensated by the telescope instrument rotator (InR). Although the focal plane of the LGS is always below the NGS focal plane, we decided to place the LGS

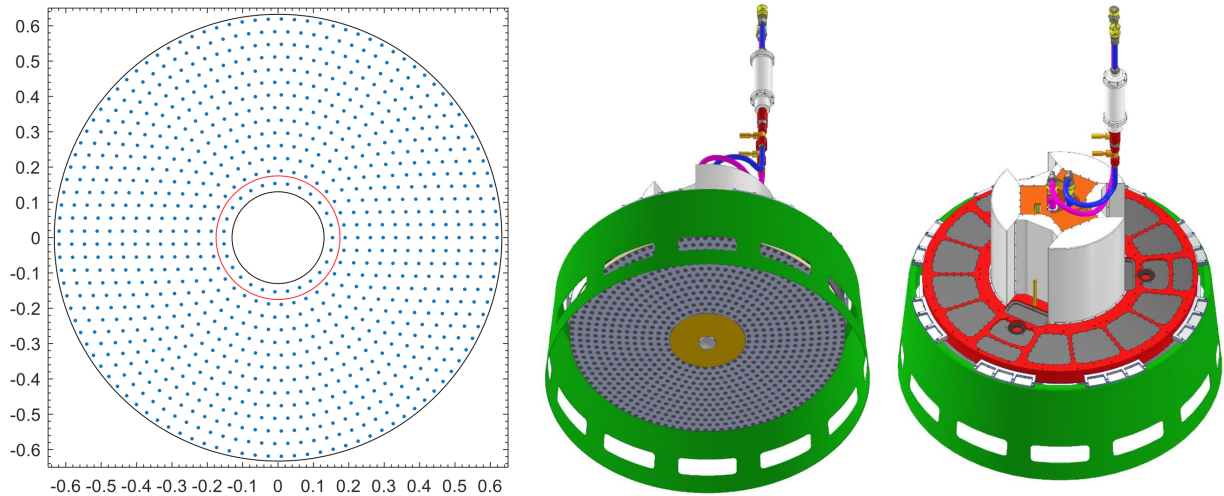


Figure 2. Left: The actuator layout of the Subaru ASM. The 924 actuators are configured over the diameter of 1,265 mm with the average spacing of 36 μm . The central 27 actuators are hidden below the center cone at the mirror surface to avoid the thermal emission from the Cassegrain hole. The hidden actuators are slaved. Right: 3D layout of the ASM unit. The unit will be installed in the existing IRM2 hexapod mount. The model is courtesy of the AdOptica consortium in Italy.

WFS layer above the NGS WFS layer to avoid the vignetting of the LGS light by the other components. The LGS WFS layer is composed by 4 Shack-Hartmann WFSs to detect the light from the 4 LGSs, each WFS has 32×32 sub-apertures for high-order wavefront correction. The NGS WFS layer is composed by 3 tip/tilt WFSs and 1 focus WFS. The NGS WFS layer detect the light from 4 NGSs. The 3 NGSs are directly imaged on the detector to correct the tip/tilt error. The light from the remaining 1 NGS is divided by 2×2 lenslet array to detect focus as well as tip/tilt so as to monitor and compensate for the slow focus offset due to the change in the LGS distance during the observation. The WFS unit is designed to acquire the 4 LGS asterism located on the circle with a radius between 2 and 10 arcmin and to acquire the 4 NGSs arbitrary located within the annulus around the science field with inner and outer radius of 7 arcmin and 10 arcmin, respectively (Figure 4).

The optical and opto-mechanical design of the WFS unit (Figure 5) has been conducted for each of the LGS WFS (32×32), the NGS WFS (1×1), and the NGS WFS (2×2). Since the WFS unit has wide patrol area for each WFS up to 10 arcmin in radius, the WFS optical system has to be designed to accommodate the change in the telescope remaining aberration and chief-ray angle. The field curvature introduces the focus offset at each WFS by changing the distance of the guide star from the field center. To minimize the focus offset and to allow us to place the field stop within the optical path of each WFS, the WFS optical system is inclined and moved along the slope that better fits the focal plane curvature (Figure 6). Moreover, the Ritchey-Chretien configuration of the Subaru telescope introduces the remaining astigmatism aberration as the guide star goes away from the field center. To remove the astigmatism aberration at any location in the guide star patrol field, each WFS has an astigmatism compensator that consists of two plates with the astigmatism surfaces. By rotating the two plates in opposite direction, the astigmatic power to compensate for the telescope remaining astigmatism aberration can be adjusted. We confirmed that the compensator can decrease the astigmatism aberration from 1.5λ to $\lambda/20$ at the edge of the WFS patrol field (10 arcmin in radius). Finally, the non-telecentricity of the telescope, which introduces the pupil shift in the WFS, is compensated for each WFS by tilting the angle of the pick-off mirror. The requirements for the WFS optical design are discussed in Ono Y. et al. in this conference.¹¹ The adopted optical and opto-mechanical design for the WFS unit are reported in more details in this conference by Tanaka, Y. et al.¹² and Martinez Rey, N. et al.,¹³ respectively.

The mechanical design of the WFS has been developed to fit within the limited envelope on the WFI support structure. The allocated area envelope is 1,750 mm in diameter and 320 mm in thickness. The 4 LGS WFSs and the 4 NGS WFSs are configured in the allocated envelope together with the WFS Adapter Flange (WAF). The

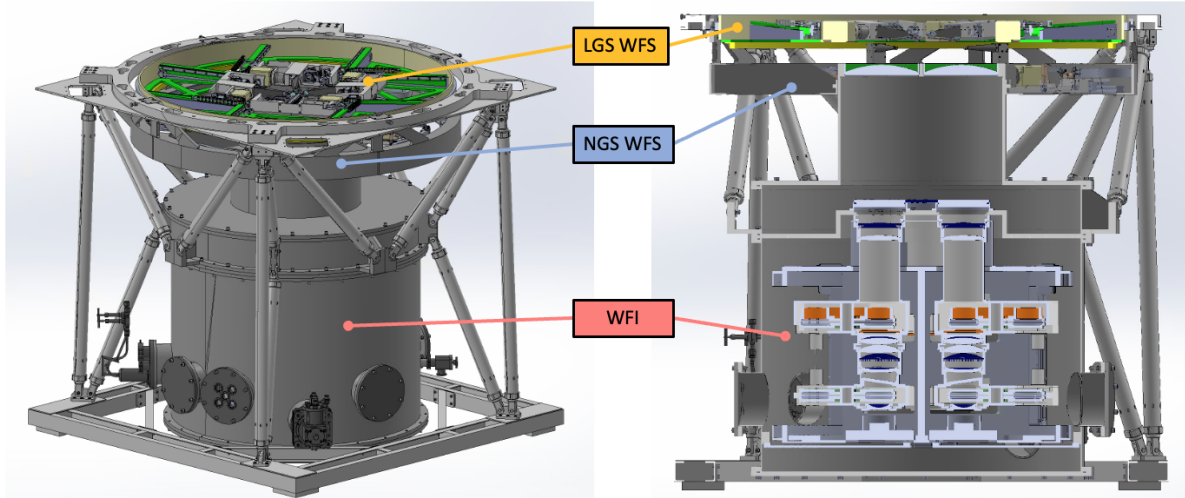


Figure 3. Left: 3D model of the GLAO WFS unit attached on top of the Cassegrain science instrument (WFI). Right: Sectional view of the model. The WFS unit that consists of the LGS WFS (upper) and the NGS WFS (lower) is attached to the Cassegrain interface ring of the WFI support structure. The WFI model is courtesy of Sumitomo Heavy Industries (SHI) and OptCraft in Japan.

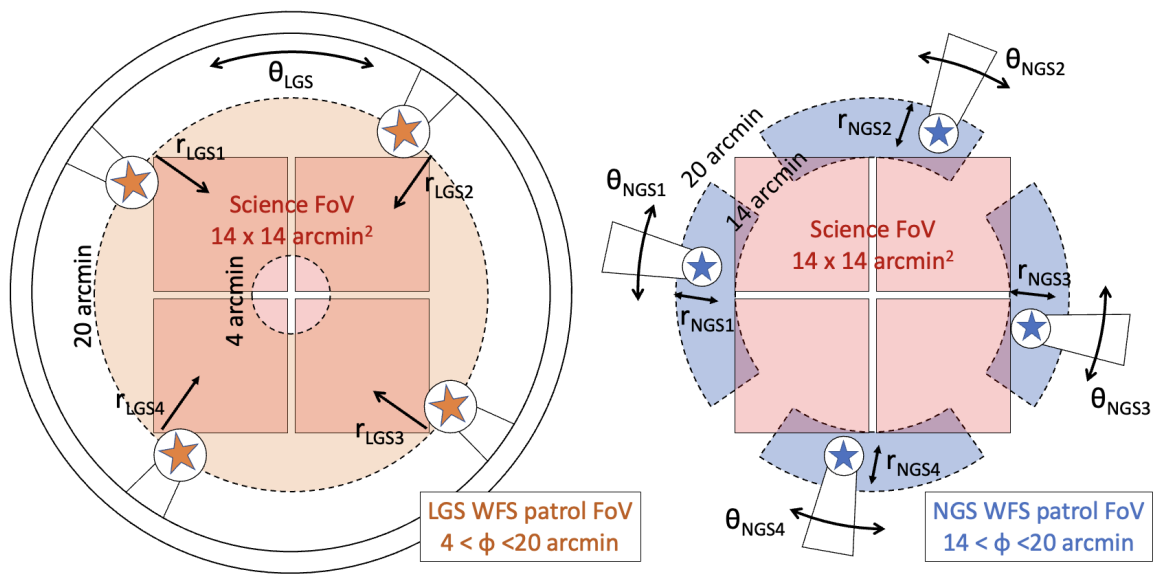


Figure 4. Guide star configuration around the science FoV of WFI at the Cassegrain. The 4 LGSs will be evenly distributed on the circle around the science FoV with a diameter between 4 and 20 arcmin (Left). The 4 NGSs are located within the $\phi = 20$ arcmin circle, but outside of the science FoV (Right). The LGS pick-off mirrors can be configured to acquire the LGSs asterism with the diameter of 4 – 20 arcmin (solid orange area) by moving individual pick-off toward radial direction. All of the LGS pick-off mirrors are moved in angular direction simultaneously. Each NGS pick-off mirror can move in radial and angular direction to acquire any NGS in the solid blue area.

NGS WAF is attached to the Cassegrain interface ring of the WFI support structure (Figure 3). The LGS WAF is carried by the NGS WAF and is equipped with a rotation mechanism. While the Cassegrain InR compensates for the field rotation for the NGS WFS and WFI, the LGS WAF needs to de-rotate the rotation by the Cassegrain InR to keep the LGSs acquired into the WFSs as the LGS asterism does not rotate with the field rotation. The entire WFS unit can be adjusted its tilt and translation with respect to WFI using the alignment mechanism at

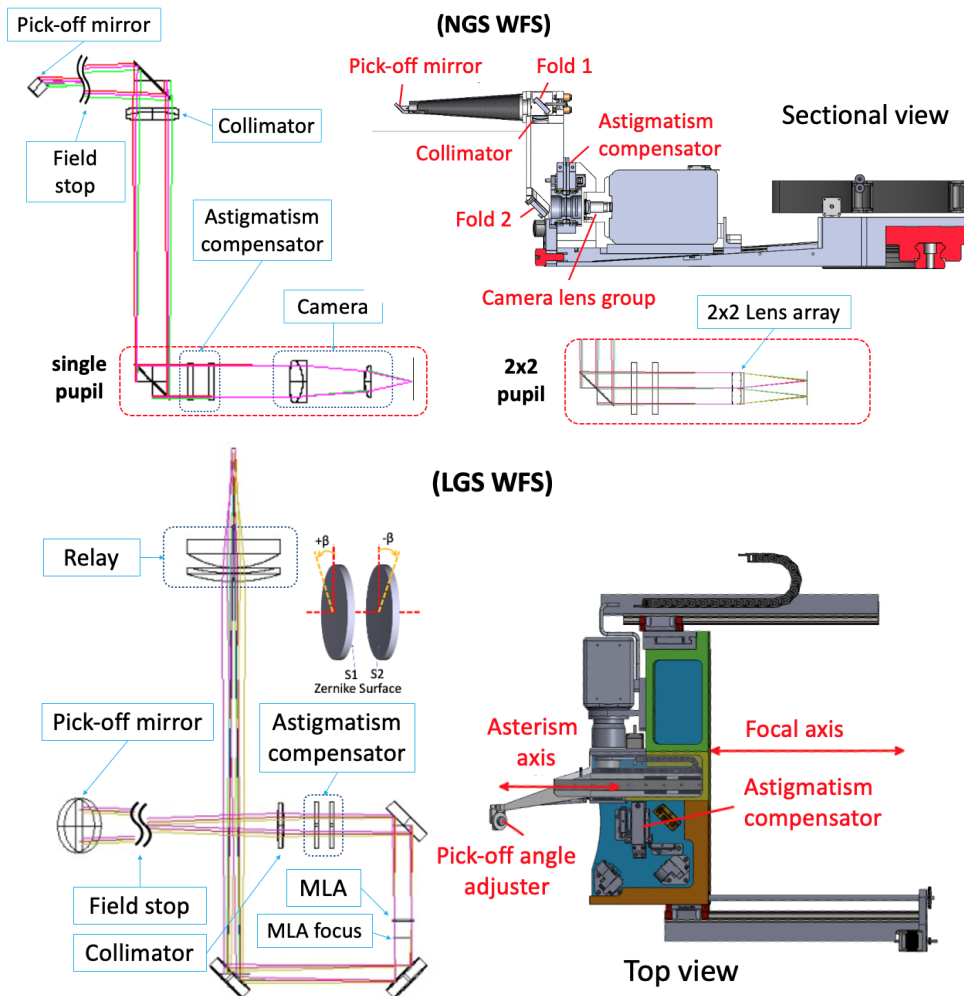


Figure 5. Optical and opto-mechanical layout of the NGS (upper) and the LGS (lower) WFSs. The optics of each WFS mainly consists a pick-off mirror that acquires the light from the NGS/LGS, a collimator lens, an astigmatism compensator, a lens array (32x32, 2x2, or none), and a camera lens unit to image on the detector.

the interface between the NGS WAF and the Cassegrain interface ring of WFI. Each LGS/NGS WFS unit can be re-configured in the WAF to acquire the guide stars located within the patrol field (Figure 4). The pick-off mirror of each LGS WFS can move in radial direction individually to acquire the LGSs on the circle between 4 and 20 arcmin in diameter. Since the four LGSs are supposed to be evenly configured on the circle, all of the LGS WFSs are rotated together by the de-rotator of the LGS WAF. The pick-off mirror of the NGS can move in radial and angular directions individually so that any NGSs in the area outside of the science FoV and within the 20 arcmin circle can be acquired.

The baseline detector selected for the WFS unit is a back-illuminated sCMOS camera from Hamamatsu Photonics (ORCA-Fusion BT). It is characterized by fast readout, low readout noise (~ 1.0 electron rms), high quantum efficiency ($\sim 95\%$ at 589 nm), and small size to fit within the limited space envelope allocated for the WFS unit. Since the selected camera is using a rolling shutter read-out scheme, each line of the image is exposed at a different time which introduce the distortion in the acquired momentary wavefront data. Due to this distortion, low-order errors in the LGS WFS can be detected as higher-order errors in the rolling shutter camera. To investigate the impact of such aliasing effect, we conducted numerical simulations and laboratory experiments using a prototype Shack-Hartmann WFS (see Section 4) and confirmed that the wavefront error

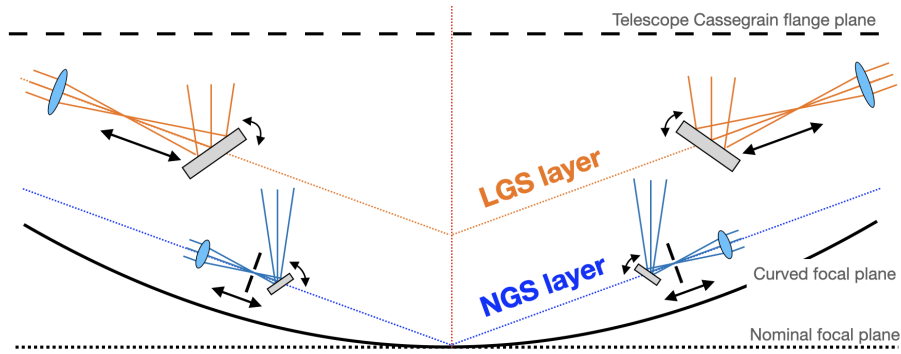


Figure 6. Schematic diagram of the WFS optical system located on the slope that fits the curved focal plane. The pick-off mirror of each WFS moves along the inclined plane to acquire the guide star in the patrol field of view. The pick-off mirror can be tilted to compensate for the difference of the chief ray angle depending on the location of the guide star.

increase due to the rolling shutter aliasing effect can be negligible in case of the GLAO. The detailed analysis and results are presented in Ogane, H. et al. in this conference.¹⁴

3.4 Laser Guide Star Facility

The laser guide star facility (LGSF) of the GLAO system will launch 4 laser beams from the laser launching telescopes (LLT) attached to the front and rear side of the center section of the Subaru telescopes. The LGSF will use two high-power (~ 20 W) 589 nm CW laser sources from the TOPTICA Projects (SodiumStar 20/2), one of which has already been deployed at the Subaru telescope to use with the existing facility Adaptive Optics system (AO188¹⁵). The laser head (LH) will be located at the front and rear side of the Subaru telescope for each, where the laser beam from the LH is splitted into two beams by using a 50/50 beam splitter, and then transferred to the LLT for each of the splitted beam. The expected photon return from the LGS is ~ 720 photon/sec/cm² assuming that 80% throughput (~ 8 W for each launched laser beam) at the launching system, 84% atmospheric throughput for both upward and downward, and 90 ph/sec/cm²/W for the photon return from the Sodium Layer expected from the simulation¹⁶ and the actual on-sky measurement¹⁷ at MaunaKea toward the optimized pointing direction. This number is also consistent with the recent measurement at the Subaru telescope during the commissioning of the TOPTICA laser (See Section 4).

The LGSF is mainly composed by the two units of the laser launching system deployed at each of the front and rear side of the telescope center section. The laser launching system includes 1 TOPTICA LH, 1 beam diagnostics system (BD), 1 beam transfer optics (BTO), and 2 LLTs (Figure 7). Two sets of TOPTICA electric cabinets (EC) are installed at the Nasmyth platform of the telescope and are connected to the LHs through the optical fibers and electric cables that are routing through the telescope elevation cable wrap. The BD system provides the capabilities of adjusting the laser power propagated to the downstream of the BD and conducting the laser beam diagnostics in terms of the laser beam alignment stability, the laser power, the beam wavefront quality, and the laser wavelength. The BD is also equipped with an alignment laser to conduct the optical alignment without using the high-power TOPTICA laser. The BTO expands the laser beam, splits the beam into two and send the each splitted beam toward the LLT, where the beam steering mirrors, one of which is a fast tip/tilt mirror (TTM) for LGS jitter control, relays the beam to the LLT. The LLT further expands the laser beam to ~ 200 mm in $1/e^2$ diameter. At the entrance of the LLT, a quarter wave plate is located to transform the laser polarization state to circular polarization at the exit of the LLT. In the LLT, a field selector mirror (FSM) is used to adjust the angle of the output laser beam to make the LGS asterism on the circle of any diameter from 0 to 20 arcmin. The LLT has more than 10 arcmin field of view to ensure the propagation of the laser beam reflected by the FSM.

The laser safety shutter is installed for each of the four laser beams so as to stop the laser propagation while slewing the telescope or the laser safety system is triggered to close the shutter for emergency reason. There is an additional laser safety shutter in the BD to stop propagating the laser to the down stream BTO. Each laser shutter is combined with the laser power meter so as to measure the laser power when the shutter is closed.

Figure 7 shows a model of the laser launching system mounted on the front side of the telescope center section. The detailed description of the model can be found in Martinez Rey, N. et al. in this conference.¹⁸

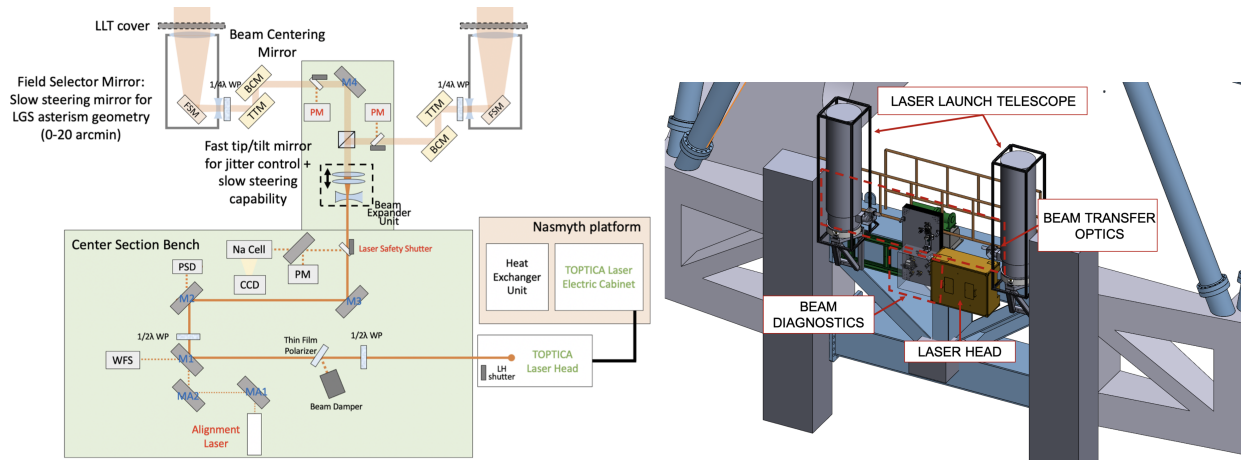


Figure 7. Left: Schematic diagram of the laser launching system. Right: Model of the laser launching system attached to the front side of the telescope center section.

3.5 Control System

The GLAO control system consists of the GLAO instrument control system (so called OBCP) and the GLAO real-time control system (RTC) as described in Figure 1. The GLAO OBCP interacts with the observation control system (OCS), send the commands to and receive the status from the GLAO hardware in non real-time manner, and send the commands to control the telescope devices through the OCS. The GLAO OBCP mainly controls the non real-time devices in the GLAO sub-system, such as the motors and stages in the WFS/LGSF that are normally used for the device initial setup and the acquisition of the guide stars before starting the AO control loop. The GLAO OBCP is also used to send the command to slowly (1-10 Hz) offload the accumulated errors in the real-time devices, such as the ASM and the LGSF fast tip/tilt mirror (TTM), to the other GLAO devices or the telescope devices that have larger range of motion.

The RTC, which collects the signals from all wavefront sensors, computes and sends the commands to the ASM and the LGSF TTM in real-time manner, will be based on the Compute and Control for Adaptive Optics (CACAO) real-time control software package.¹⁹ The frame rate of the LGS WFS is 500 Hz. The frame rate of the NGS WFS is less than 500 Hz and it changes depending on the brightness of the NGSs. Figure 8 shows the schematic diagram of the GLAO control loop. The WFS images are processed at the WFS sub-systems and the computed sub-aperture slopes or tip/tilt errors are transferred to the GLAO RTC. The LGS WFS slope data is processed first to derive the differential rotation between the LGS WFS de-rotator and the telescope InR, to extract the tip/tilt error from each LGS WFS slope data, and then to compute the high-order modes (focus or higher up to ~ 350 modes) for each WFS. The high-order modes from the four LGS WFSs are averaged and multiplied by the interaction matrix (IM) to derive the ASM high-order modes. The extracted differential rotation is used to slowly offload the rotation error by giving the offset to the LGS WFS de-rotator. The tip/tilt errors from each LGS WFS are used for the LGS jitter compensation at the corresponding laser launching system by moving the TTM in real-time manner. The data from the NGS WFS is processed to decompose the tip/tilt and the focus modes from the 2x2 NGS WFS, extract the differential rotation between the field rotation and the InR angle, and then extract the tip/tilt modes for each NGS WFSs. The tip/tilt modes from the four NGS WFSs are averaged and multiplied by the tip/tilt IM to derive the ASM tip/tilt mode. The computed ASM high-order and tip/tilt modes are transferred to the ASM in the real-time manner to deform the shape of the ASM. The 2x2 NGS WFS can measure the focus offset due to the change in the LGS distance either by the telescope EL motion or the Sodium layer height fluctuation. The defocus mode measured by the 2x2 NGS WFS is compensated by moving the focus stage of the LGS WFSs.

In addition to the main control loop, there are several slow offloading loops to remove the accumulated low-order errors from the real-time devices. The tip/tilt mode accumulated on the ASM can be offloaded by moving the telescope Az/EL mount. The defocus and coma mode can be offloaded by translating the secondary mirror position in (x,y,z) directions with the IRM2 hexapod.

The real-time telemetry data from the WFS measurements and the ASM mirror shape are stored and used to compute a pseudo synthetic interaction matrix²⁰ as needed when the mis-registration between the WFS and the ASM occurs.

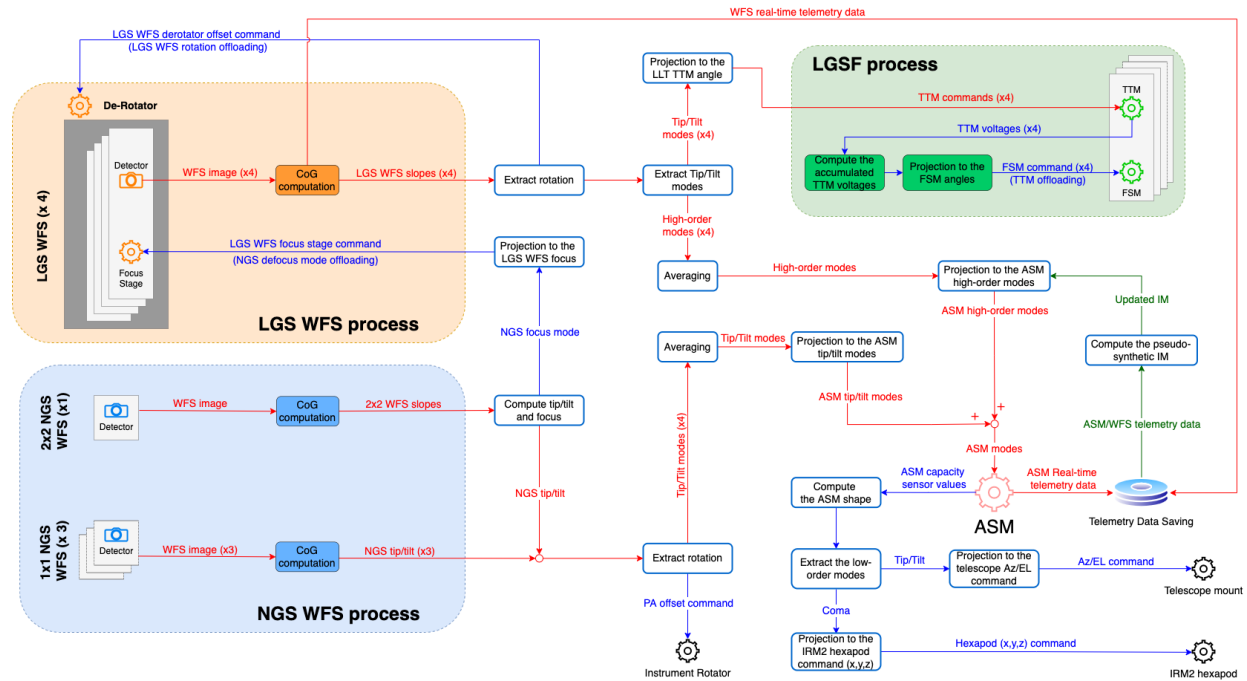


Figure 8. GLAO control loop diagram. Red-lines show the real-time signals/commands, while blue lines show the non real-time signals/commands mainly used for slow offloading loop. Green lines indicate the signals/commands that are processed as needed. Non-colored blocks show the processes involved in the GLAO RTC. Colored blocks show the processes in each GLAO sub-system.

4. PROTOTYPING ACTIVITIES

To validate the design selected for the GLAO system, we have been developing the prototype instruments to test at the Subaru telescope. ULTIMATE-START is a Laser Tomography Adaptive Optics (LTAO) system to be implemented in the existing Subaru facility AO system (AO188). It uses four Shack-Hartmann (SH) WFSs with the same 32x32 sub-apertures as the LGS WFS for the GLAO system to reconstruct the tomographic wavefront error using 4 LGSs. The four SH-WFS system has been fully fabricated and is currently being tested at Tohoku University. We have recently commissioned the new LGSF at the Subaru telescope with the TOPTICA laser for ULTIMATE-START. The laser and its diagnostic system has been installed at the front side of the telescope center section as we are planning for the GLAO LGSF, demonstrating the technical feasibility of the GLAO LGSF. The RTC of ULTIMATE-START will be fully compatible with the GLAO system so that we can use ULTIMATE-START as a testbed for the GLAO RTC. ULTIMATE-START will be installed at the Subaru telescope in late 2022 and start the commissioning in early 2023. Not only for the purpose of the GLAO key technology prototyping, ULTIMATE-START will provide the Subaru community with a new capability of high Strehl ratio AO correction especially in visible wavelength with the aid of the LTAO. Current status of ULTIMATE-START is discussed in Terao, K. et al. in this conference.²¹

We have also developed a single SH-WFS to validate the sCMOS rolling shutter read-out mode with the LGS. It is equipped with a 32x32 sub-apertures and the sCMOS camera from the Hamamatsu Photonics to acquire the light from the single LGS generated by the new LGSF with the TOPTICA laser. The single SH-WFS has been installed after AO188 and tested with the LGS during the commissioning run of the new LGSF in early 2022. The impact of the rolling shutter aliasing effect onto the wavefront reconstruction has been evaluated with the SH-WFS, which is reported by Ogane, H. et al. in this conference.¹⁴

The performance of the GLAO system has been estimated based on the end-to-end numerical simulation³ using the Maunakea Cn² profile from the literature.^{22,23} However, the ground layer turbulence, which seriously affects the GLAO performance, has not been measured from the Subaru telescope. To estimate the ground-layer turbulence, we have been developing a turbulence profiler to install at the Subaru Nasmyth platform. The profiler is composed by two SH-WFSs to observe separated stars and recovers the turbulence altitude profile up to around 100 m using the SLODAR method.²⁴ The profiler has been assembled and implemented at the Subaru Nasmyth focus. We are planning to obtain the data with the profiler in late 2022.

5. CONCLUSIONS

We presented the design overview of the GLAO system for ULTIMATE-Subaru that allows us to obtain the uniform seeing improvement up to 20 arcmin in diameter at the Cassegrain focus of the Subaru telescope to use with the dedicated NIR wide-field imager (WFI). The design of the GLAO subsystems (ASM, WFS, LGSF, and control system) have been validated, demonstrating the capabilities to conduct new wide-field NIR survey programs with the GLAO assisted sensitivity and spatial resolution. The GLAO system is currently at the end of the preliminary design phase, while the prototyping activities to validate the selected design are ongoing. Following the GLAO development schedule, the first light of the GLAO system will be expected in 2028 time frame.

ACKNOWLEDGMENTS

We appreciate the National Astronomical Observatory of Japan (NAOJ) and the ULTIMATE-Subaru science team, which consists of astronomers not limited to Japan, for financially, technically, and scientifically supporting the ULTIMATE-Subaru project. ULTIMATE-Subaru project is financially supported by the FY2021 supplementary budget from the Japanese Ministry of Education, Culture, Sports, Science and Technology (MEXT). This work is also supported by the JSPS Core-to-Core Program (grant number: JPJSCCA20210003).

REFERENCES

- [1] Miyazaki, S., Komiyama, Y., Kawanomoto, S., et al., “Hyper Suprime-Cam: System design and verification of image quality,” *PASJ* **70**, S1 (2018).
- [2] Tamura, N., Moritani, Y., Yabe, K., et al., “Prime Focus Spectrograph (PFS) for the Subaru telescope: Its start of the last development phase,” in [*Ground-based and Airborne Instrumentation for Astronomy IX*], Evans, C. J., Bryant, J. J., and Motohara, K., eds., *Proc. SPIE*, 12184–36 (2022).
- [3] Rigaut, F., Minowa, Y., Akiyama, M., et al., “A conceptual design study for Subaru ULTIMATE GLAO,” in [*Adaptive Optics Systems VI*], Close, L. M., Schreiber, L., and Schmidt, D., eds., *Proc. SPIE* **10703**, 692 – 706 (2018).
- [4] Motohara, K., Minowa, Y., Tanaka, I., et al., “ULTIMATE-Subaru: conceptual design of WFI, a near-infrared wide field imager,” *Proc. SPIE* **11447**, 99 – 108 (2020).
- [5] Suzuki, R., Tokoku, C., Ichikawa, T., Uchimoto, Y. K., Konishi, M., Yoshikawa, T., Tanaka, I., Yamada, T., Omata, K., and Nishimura, T., “Multi-Object Infrared Camera and Spectrograph (MOIRCS) for the Subaru Telescope I. Imaging,” *PASJ* **60**, 1347–1362 (Dec. 2008).
- [6] Minowa, Y., Koyama, Y., Yanagisawa, K., et al., “ULTIMATE-Subaru: system performance modeling of GLAO and wide-field NIR instruments,” in [*Modeling, Systems Engineering, and Project Management for Astronomy IX*], Angeli, G. Z. and Dierickx, P., eds., *Proc. SPIE* **11450**, 178 – 189 (2020).

- [7] Ono, Y., Akiyama, M., Terao, K., Minowa, Y., Ogane, H., and Oya, S., “Covariance-based analytical algorithm to predict the performance of tomographic AO systems,” in [*Adaptive Optics Systems VIII*], Schreiber, L., Schmidt, D., and Vernet, E., eds., *Proc. SPIE*, 12185–15 (2022).
- [8] Biasi, R., Gallieni, D., Salinari, P., Riccardi, A., and Mantegazza, P., “Contactless thin adaptive mirror technology: past, present, and future,” in [*Adaptive Optics Systems II*], Ellerbroek, B. L., Hart, M., Hubin, N., and Wizinowich, P. L., eds., *Proc. SPIE* **7736**, 872 – 885 (2010).
- [9] Andrighttoni, M., Biasi, R., Manetti, M., Tintori, M., Thompson, P. M., Spanos, J., and Bouchet, A., “GMT ASM prototype dynamic and optical tests results,” in [*Adaptive Optics Systems VIII*], Schreiber, L., Schmidt, D., and Vernet, E., eds., *Proc. SPIE*, 12185–300 (2022).
- [10] Oya, S., Minowa, Y., Okita, H., Ono, Y., and Clergeon, C., “ULTIMATE-Subaru: adaptive secondary mirror system,” in [*Adaptive Optics Systems VIII*], Schreiber, L., Schmidt, D., and Vernet, E., eds., *Proc. SPIE*, 12185–295 (2022).
- [11] Ono, Y., Minowa, Y., Tanaka, Y., et al., “ULTIMATE-Subaru : Requirement analysis of the WFS system for GLAO,” in [*Adaptive Optics Systems VIII*], Schreiber, L., Schmidt, D., and Vernet, E., eds., *Proc. SPIE*, 12185–125 (2022).
- [12] Tanaka, Y., Minowa, Y., Ono, Y., et al., “ULTIMATE-Subaru: adaptive secondary mirror system,” in [*Adaptive Optics Systems VIII*], Schreiber, L., Schmidt, D., and Vernet, E., eds., *Proc. SPIE*, 12185–295 (2022).
- [13] Martinez Rey, N., Herrald, N., Chandler, D., et al., “Wavefront sensing over a 20-arcmin field in the ULTIMATE-Subaru Ground Layer Adaptive Optics system,” in [*Adaptive Optics Systems VIII*], Schreiber, L., Schmidt, D., and Vernet, E., eds., *Proc. SPIE*, 12185–249 (2022).
- [14] Ogane, H., Akiyama, M., Cranney, J., et al., “Aliasing effect of rolling shutter readout in laser guide star wavefront sensing,” in [*Adaptive Optics Systems VIII*], Schreiber, L., Schmidt, D., and Vernet, E., eds., *Proc. SPIE*, 12185–22 (2022).
- [15] Minowa, Y., Hayano, Y., Terada, H., et al., “Subaru laser guide adaptive optics system: performance and science operation,” in [*Adaptive Optics Systems III*], Ellerbroek, B. L., Marchetti, E., and Véran, J.-P., eds., *Proc. SPIE* **8447**, 84471F (July 2012).
- [16] Holzlöhner, R., Rochester, S. M., Bonaccini Calia, D., et al., “Optimization of cw sodium laser guide star efficiency,” *A&A* **510**, A20 (Feb. 2010).
- [17] Chin, J. C. Y., Wizinowich, P., Wetherell, E., et al., “Keck II laser guide star AO system and performance with the TOPTICA/MPBC laser,” in [*Adaptive Optics Systems V*], Marchetti, E., Close, L. M., and Véran, J.-P., eds., *Proc. SPIE* **9909**, 254 – 272 (2016).
- [18] Martinez Rey, N., Kruse, A., Herrald, N., et al., “Preliminary design of the Laser Guide Star Facility for the ULTIMATE-Subaru Ground Layer Adaptive Optics system,” in [*Adaptive Optics Systems VIII*], Schreiber, L., Schmidt, D., and Vernet, E., eds., *Proc. SPIE*, 12185–281 (2022).
- [19] Guyon, O., Sevin, A., Gratadour, D., et al., “The compute and control for adaptive optics (CACAO) real-time control software package,” in [*Adaptive Optics Systems VI*], Close, L. M., Schreiber, L., and Schmidt, D., eds., *Proc. SPIE* **10703**, 469 – 480 (2018).
- [20] Kolb, J., “Review of AO calibrations, or how to best educate your AO system,” in [*Adaptive Optics Systems V*], Marchetti, E., Close, L. M., and Véran, J.-P., eds., *Proc. SPIE* **9909**, 200 – 206 (2016).
- [21] Terao, K., Akiyama, M., Minowa, Y., et al., “ULTIMATE-START: current status of the Subaru Tomography Adaptive optics Research experiment project,” in [*Adaptive Optics Systems VIII*], Schreiber, L., Schmidt, D., and Vernet, E., eds., *Proc. SPIE*, 12185–250 (2022).
- [22] Chun, M., Wilson, R., Avila, R., Butterley, T., Aviles, J.-L., Wier, D., and Benigni, S., “Mauna Kea ground-layer characterization campaign,” *MNRAS* **394**, 1121–1130 (Apr. 2009).
- [23] Els, S. G., Travouillon, T., Schöck, M., Riddle, R., Skidmore, W., Seguel, J., Bustos, E., and Walker, D., “Thirty Meter Telescope Site Testing VI: Turbulence Profiles,” *PASP* **121**, 527 (May 2009).
- [24] Wilson, R. W., “SLODAR: measuring optical turbulence altitude with a Shack-Hartmann wavefront sensor,” *MNRAS* **337**, 103–108 (Nov. 2002).